Received: 10 January 2022 | Revised: 14 March 2022 | Accepted: 29 May 2022

DOI: 10.1002/app.52761

RESEARCH ARTICLE

Applied Polymer SCIENCE WILEY

Polysaccharide-based electroconductive films for controlled release of ciprofloxacin

Didem Aycan | **Nihal Dolapçı** | **Özge Gülüzar Karaca** | **Neslihan Alemdar**

Marmara University, Department of Chemical Engineering, Istanbul, Turkey

Correspondence
Neslihan Alemdar, Marmara University, Department of Chemical Engineering, 34722, Istanbul, Turkey.
Email: neslihan.alemdar@marmara.edu.tr

Abstract

Hereby, fabrication of hyaluronic acid/gelatin/sodium alginate (HA/Gel/SA) polymeric films, which contain electroconductive poly(3,4ethylenedioxythiophene)/poly(styrenesulfonate) (PEDOT:PSS) particles, is studied for drug release applications. The characterization of synthesized PEDOT:PSS and HA/Gel/SA-(PEDOT:PSS) films is verified by using FT-IR and RAMAN spectroscopy. Conductivity values of the films containing 0, 4, and 6% v/v PEDOT:PSS are found via a four-point probe technique to determine the optimum composition of the films for the targeted field. Additionally, swelling, mechanical, and cytotoxicity tests are carried out according to the related methods. Ciprofloxacin (CIP), which is a commonly used antibiotic, is loaded into the polymeric matrix and its release behavior is investigated. All results indicate that the incorporation of PEDOT:PSS increases the mechanical performance and decreases the burst release of drug resulted in more sustained release profile. The HA/Gel/SA-(PEDOT: PSS) formulation is clearly a promising drug carrier that also supports cell viability due to its high cytocompatibility.

KEYWORDS

conducting polymers, drug delivery systems, polysaccharides

1 | INTRODUCTION

In recent years, electroconductive polymeric films based on the polysaccharides have been increasingly used to produce drug carriers for controlled release applications, since the strong combination of conductivity and biocompatibility provides a more controlled release rate and profile in the targeted region as well as supports cell proliferation, growth, and intercellular electrical interactions.[1–8] This combination provides not only the electro-sensitive nature, that is a crucial requirement especially for the transdermal drug release, but also repeatability of the delivered flux due to the redox properties of electroconductive networks.[9,10] Drug release systems based on the electroconductive structures promote the binding and releasing of drugs through electrostatic interactions, that leads to modulated drug release patterns with electrical stimulation.[9] Additionally, the formation of electroconductive networks could improve the mechanical stability of the drug carriers so they reach the targeted region by acting as a filler material.[10–12] Among the conductive polymers, poly(3,4-ethylenedioxythiophene) (PEDOT) is one of the most promising conductive polymers, which has been used in the formation of the electroactive biomaterials.[13–16] Although PEDOT has excellent properties, including high conductivity, ease of synthesis and good thermal and oxidative stability, it is insoluble in many solvents.[17–19] This drawback could be eliminated by doping of PEDOT with poly(styrenesulfonate) (PSS) to create a water-soluble structure with good film-forming properties. Additionally, using of the PEDOT:PSS in a polymeric network as a

filler material gives the possibility to enhance the mechanical strength of the structure. Despite all these, the low bio-functionality and biocompatibility of PEDOT:PSS restricts its usage in the biomaterial applications.[20] Therefore, the incorporation of PEDOT:PSS within the polysaccharides such as hyaluronic acid, gelatin, sodium alginate, chitosan, collagen, and cellulose was mostly preferred in the production of electroconductive materials, since these biomaterials have desirable bioactivity and they improve the biocompatibility and biodegradability of the structure.[21] In the current study, the electroconductive polymeric film was fabricated by incorporating conductive PEDOT:PSS into the sodium alginate (SA), hyaluronic acid (HA), and gelatin (Gel)-based polymeric network for its potential usage as a drug carrier. SA, whose structure consists of 1,4-linked β-D mannuronic acid and α-L-guluronic acid units, is a natural and nontoxic polysaccharide. It has been commonly used for various drug delivery systems, because the functional groups of the structure enable to easily modification.[22–25] HA which was used as an anionic polysaccharide, is composed of repeating N-acetyl glucosamine and glucuronic acid units, possesses the property of the polyelectrolyte and has an ability to enhance the interfacial hydration.[26–29] Additionally, it shows excellent properties such as biocompatibility, biodegradability, and being antifouling towards proteins.[30–34] Therefore, there are many reports involving the controlled drug release from HA and HA-based polymeric networks.[35] However, poor mechanical performance of HA causes us to limit the application fields that need the protection of the material integrity.[36–38] The fabrication of HA-based polymeric networks, which includes other biopolymer components, can offer significant advantages compared to the single use of HA, since the mechanical performance and stability are crucial in these type of applications as well as non-toxicity and biocompatibility.[39–41] A possible approach to improve the mechanical performance is the modification of HA with Gel due to its mechanical stability and good film forming ability.[36,37,42,43] Gel is produced by partial hydrolysis of collagen and has been widely preferred in biomaterial production owing to its good bioactivity.[44–48] Furthermore, Gel generates outstanding cell responses because of its arginine-glycine-aspartic acid sequences supported cell attachment and proliferation.[49–52] As a result of these, it should be clear that the combination of these three polysaccharides might create a desired polymeric network with brilliant properties coming from each of the components. The structural analysis, electrical conductivity, swelling performance, and mechanical properties of obtained HA/Gel/SA-(PEDOT:PSS) polymeric films were evaluated, as well as cytotoxicity regarding as the aimed application field. Ciprofloxacin (CIP), which has a high efficacy against most of the bacterial pathogens, including gram-positive and gram-negative bacteria, was selected as the model antibiotic drug.[53–57] CIP was loaded into the electroconductive polymeric films to investigate their usage as a drug carriers. Following that, the release studies were performed. Many researchers have focused on producing polymeric networks by using different polysaccharides for the controlled release of CIP. In particularly, the binary combination of the polymers is considered as more favorable to achieve desirable properties.[58] A number of studies have demonstrated drug carriers for sustained release of CIP via blending of two polymers including Gel, SA, HA, and chitosan in order to eliminate insufficient features such as sensitivity to degradation, poor flexibility and mechanical stability depending on the aimed application field.[59–64] Considering all of these, the ternary combination of HA/Gel/SA was prepared in the current study to obtain the drug carrier with improved physico-mechanical characteristics compared to the polymeric network formed by the binary polymer combination or the individual polymer. The drug release results indicated that the CIP release from the HA/Gel/SA-(PEDOT:PSS) polymeric film occurred in a more controlled manner with a slower release rate compared with the previous studies in the literature, since this formulation formed a stronger network, where the drug molecules are encapsulated. The findings of this study proved that the produced HA/Gel/SA-(PEDOT:PSS) electroconductive polymeric film formulation might be potentially used as a drug carrier to provide a favored network with great cytocompatibility, improved mechanical performance, and controlled release profile for drug delivery systems.

2 | EXPERIMENTAL

2.1 | Materials

Hyaluronic acid (HA, food grade, $M_W = 8 \times 10^5$ Da), gelatin (Gel, medical grade, 280–320 bloom, Type A), sodium alginate (SA, medical grade, viscosity 250 cps, 25°C), and 1-Ethyl-(3-3-dimethylaminopropyl) carbodiimide (EDC) were purchased from Heze Better Biochemical Co., Ltd. (China). 3,4 ethylenedioxythiophene (EDOT), iron (III) nitrate nonahydrate ($Fe[NO_3]_3.9H_2O$), poly(sodium-4-styrene sulfonate) (NaPSS), phosphate buffer saline (PBS) tablet, ciprofloxacin ($C_{17}H_{18}FN_3O_3$), and ethanol (EtOH) were obtained from Sigma Aldrich. Cell culture chemicals and solutions including medium (Dulbecco's Modified Eagle Medium-Roswell Park Memorial Institute, DMEM-RPMI), antibiotic, trypsin,

fetal bovine serum (FBS) were purchased from PAN Biotech (Germany). (4-[3-(4-iodophenyl)-2-(4-nitrophenyl)-2H-5-tetrazolio] 1,3 benzenedisulfonate) (WST-1) cell proliferation reagent was provided by Roche (Switzerland). L929 (Murine Fibroblasts) cell lines were received as gifts from Prof. Julide Akbuga (Marmara University). All the chemicals were used without any purification.

2.2 | Synthesis of PEDOT:PSS

EDOT (0.8 ml) was dispersed into a 0.1 M NaPSS solution (15 ml), and the obtained solution was mixed for 30 min at room temperature. Then, $Fe(NO_3)_3.9H_2O$ (15.3 g) was dissolved in distilled water (5 ml) and added into the solution. The reaction was carried out under continuous stirring for 2 h. The product was collected via centrifugation at 6500 rpm for 10 min. Following that, the precipitate was cast into a petri dish and dried at 50°C under a vacuum for 24 h.

2.3 | Fabrication of HA/gel/SA-(PEDOT:PSS) conductive films

HA/Gel/SA-(PEDOT:PSS) conductive films were fabricated by the solvent casting evaporation method. The stock polymer solution was obtained by dissolving HA, Gel, and SA in distilled water (1% w/v) with a proportion of 10, 45, and 45%, respectively. The PEDOT:PSS suspension was prepared in PBS (0.1% w/v) by ultrasonic treatment for 10 min and the different amounts of this suspension (4 and 6 v%) were added into the stock polymer solution. EDC dissolved in EtOH (0.5% w/v) was added into the obtained mixtures as a coupling agent. Finally, all mixtures were dried in petri dishes at 37°C for 3 days.

2.4 | Characterization

While the HA/Gel/SA-(PEDOT:PSS) conductive films were characterized by Fourier transform infrared spectroscopy (FT-IR), the chemical structure of PEDOT:PSS was verified by FT-IR and RAMAN spectroscopy. FT-IR analyses were carried out using a Perkin Elmer Spectrum One FT-IR with an attenuated total reflectance (ATR) unit in the scanning range of 500–4000 cm^{-1}. A Raman analysis was recorded with a STEX-100 Compact Confocal Raman spectrometer with a laser at 532 nm as the excitation source. The surface morphologies of the polymeric films sputter coated with Au/Pd were investigated using scanning electron microscopy (SEM) (ZEISS EVO MA10).

2.5 | Electrical conductivity of HA/gel/SA-(PEDOT:PSS) films

The electrical conductivity of the films (4% and 6% PEDOT:PSS v/v) was determined by using Lucas Labs S-302 Four Point Resistivity Probing Equipment which was connected to a Gamry Instrument power source in order to supply the constant current and to read the operating voltage. Sheet resistivity (ρ) was found by using Equation (1);

$$\rho = \frac{\pi t V}{\ln 2 I} \tag{1}$$

where t (cm) is the film thickness, V (V) is the potential difference between the two inner probes, and I (A) is the current through the outer pair of probes. Then, the conductivity (σ) values of the films were calculated by using Equation (2);[65]

$$\sigma = \frac{1}{\rho} \tag{2}$$

2.6 | Swelling properties

The water uptake capacity of HA/Gel/SA-(PEDOT:PSS) films (0% and 4% v/v PEDOT:PSS) was evaluated by swelling the films in pH 7.4 buffer solution at 37°C for 24 h in an orbital shaker-incubator and measuring the weight difference of dry and swollen films gravimetrically. Following that, the swelling ratio (SR) of the films was determined according to Equation (3);

$$SR(\%) = \frac{W_s - W_d}{W_d} \times 100 \tag{3}$$

where W_d and W_s are the weight of the films before and after swelling, respectively.

2.7 | Mechanical performance

The mechanical performance of film samples was tested by using a universal testing machine (Zwick Z010 universal tensile tester, Kennesaw, GA) equipped with a 0.01 N load cell and 2 mm/min crosshead speed. Film specimens were cut to the same dimensions as a rectangular

forms (1 × 5 cm). Three film samples were tested for each condition at room temperature and the average values were recorded. The results were evaluated in terms of tensile strength (MPa), elastic modulus (N/mm^2), and elongation at break (%). Tensile strength and elongation at break were calculated by Equation (4) and Equation (5) respectively;

$$TS = \frac{F_{max}}{A} \quad (4)$$

$$E(\%) = \frac{L}{L_0} \times 100 \quad (5)$$

where F_{max} (N) and A (mm^2) correspond to the maximum force at break and the cross-sectional area of the specimen, respectively. L (mm) is the final length of the film sample at rupture, and L_0 (mm) represents the original length of the film sample prior to the mechanical test.

2.8 | Cytotoxicity tests

Cytotoxicity of the film samples was investigated by WST-1 cell proliferation and viability assay with the L929 cell line (Murine Fibroblast) according to the protocol described precisely in our previous study.[66] The measurements were carried out by comparing the number of viable cells (WST-1) between a sample-free control group and a seeded sample. The absorbance value of WST-1 for each sample was determined spectrophotometrically at 450 nm by using a Promega Glomax-Multi + detection system.

2.9 | Drug loading and in vitro release studies

The film samples, precut into 1 cm^2 dimensions, were swollen in a 500 ppm CIP drug solution for 3 days. Drug loaded film samples were taken out of from the solution and washed with distilled water (3 ml) in order to remove any excess of drug on the surface of the film samples. Following that, the film samples were dried at room temperature for 24 h. The drug loaded-dried film samples were immersed into the falcon tubes containing of buffer solutions (15 ml) at 37°C for incubation (at 130 rpm). During the release process, the solution (3 ml) was withdrawn and replaced with the same amount of fresh buffer solution at predetermined time intervals to provide a constant volume release medium. The releasing amount of CIP from the film samples was followed by measuring the intensity of the UV absorbance at 270 nm using an UV–vis spectrophotometer (Agilent Cary 60 Spectrophotometer).

2.10 | Statistical analyses

Statistical analysis was done and reported as a mean ± standard deviation (SD) by using GraphPad Prism Software (V.5, San Diego, USA) including one-way ANOVA. A Tukey test was performed as a comparison test. The results were expressed as means ±standard deviation (SD) and significance was defined as a p-value<0.05.

3 | RESULTS AND DISCUSSION

3.1 | Synthesis of PEDOT:PSS

PEDOT:PSS was synthesized by means of the oxidative reaction, which was depicted in Figure 1. In the first step, NaPSS acted as the oxidizing agent, dissociating into sulfate radicals and sodium ions. Following that, oxidation of EDOT monomers occurred, which resulted in the formation of EDOT radicals. The protons which were generated by the coupling of EDOT radicals were removed in the propagation step, while the sulfate ions and PSS chains could interact with the formed PEDOT chains via electrostatic forces and interchain entanglements. At the end of the polymerization, the color transformation arising from the chromic nature of the PEDOT was used as an indication to confirm the formation of PEDOT:PSS.[4,67]

3.2 | Fabrication of HA/gel/SA-(PEDOT:PSS) conductive films

In the present study, PEDOT:PSS-reinforced electroconductive polymeric films including biocompatible constituents (HA, Gel, and SA) were fabricated to overcome the challenges related to the complex usage of drugs, since the nature of these types of electroconductive polymeric films enables to control of release rate and profile (Figure 2).[1,68,69]

As shown in Figure 3, while the pure film was transparent, the color of films containing PEDOT:PSS became darker owing to the incorporation of PEDOT:PSS into the polymeric network. Due to its less cytotoxic nature compared to conventional ones, EDC was employed as the coupling agent to support an environmentally friendly synthesis approach.[70] Furthermore, the usage of Gel in the ternary network enabled to obtain mechanically strong and flexible polymeric films as expected.

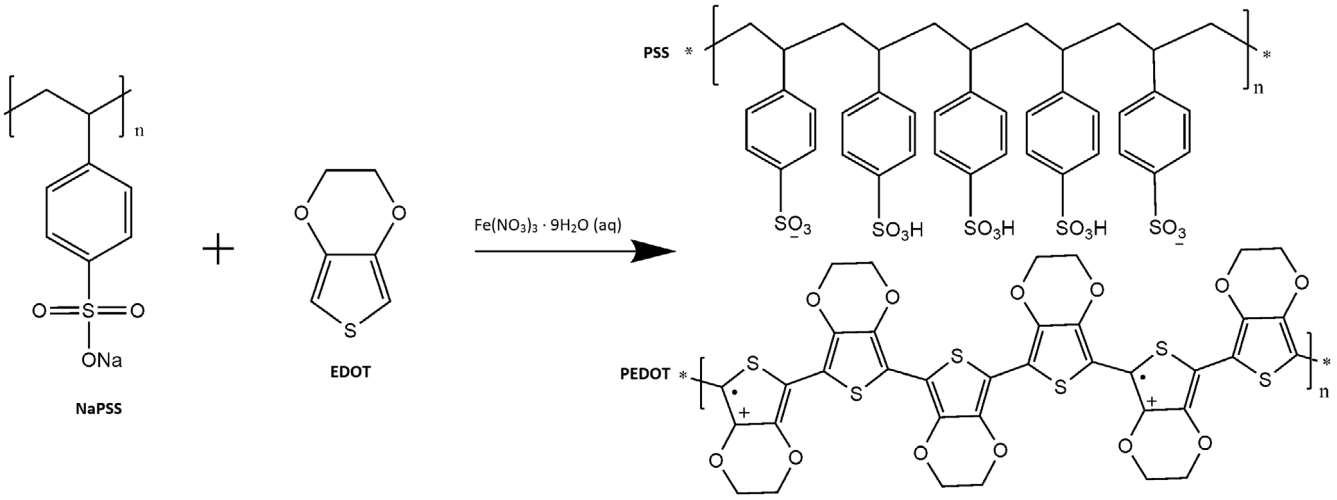

FIGURE 1 Reaction mechanism of synthesis of PEDOT:PSS

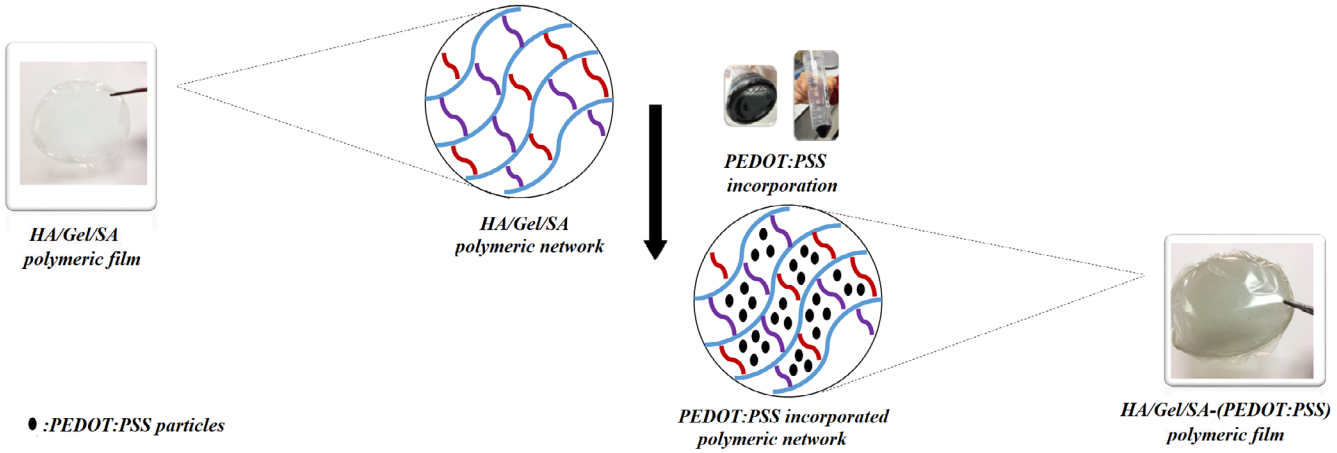

FIGURE 2 Schematic diagram of producing HA/gel/SA-(PEDOT:PSS) polymeric film [Color figure can be viewed at wileyonlinelibrary.com]

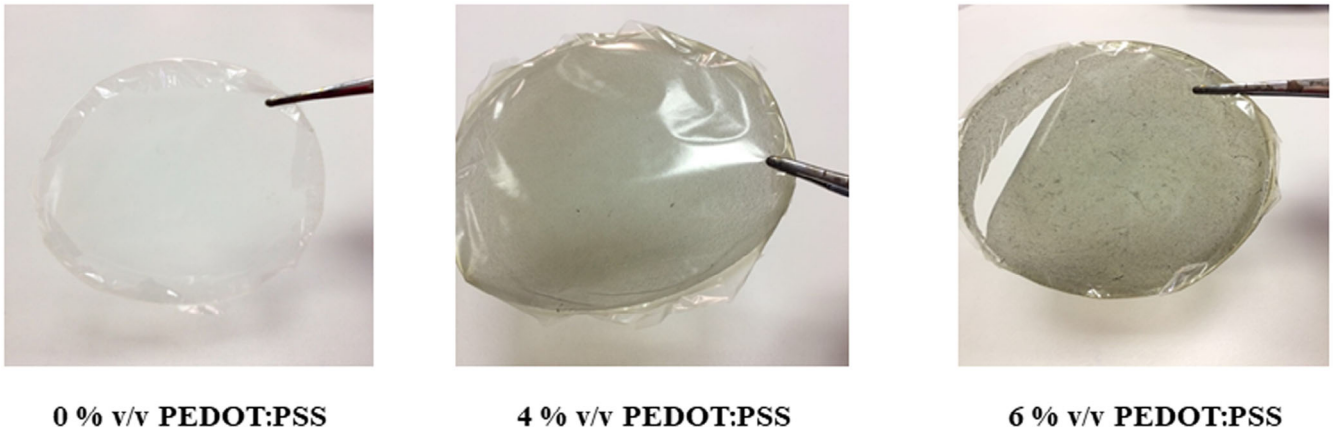

FIGURE 3 Images of fabricated polymeric films with different amount of PEDOT:PSS [Color figure can be viewed at wileyonlinelibrary.com]

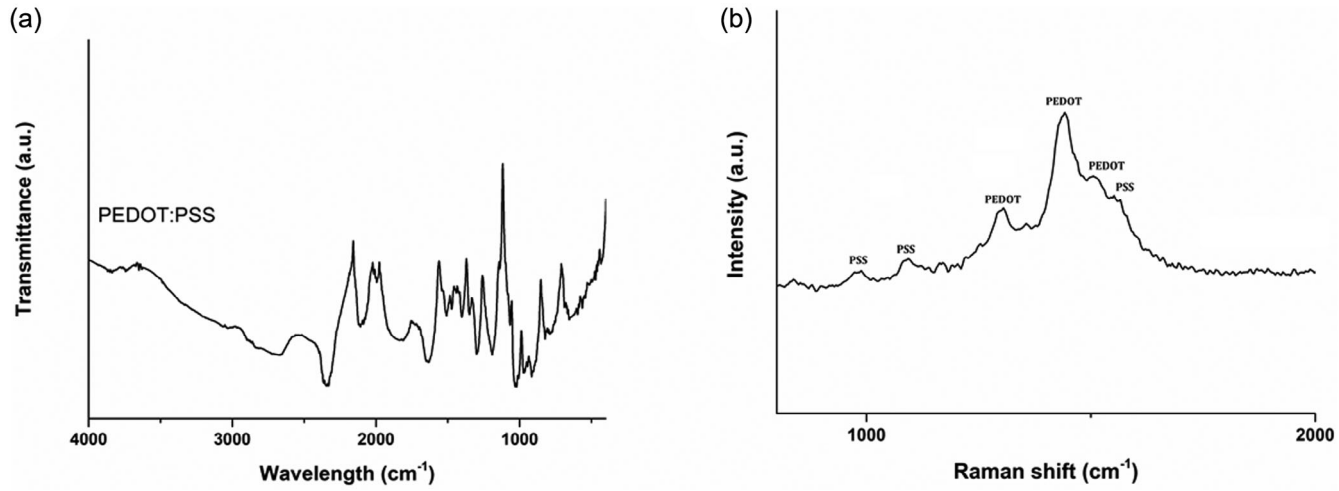

FIGURE 4 FT-IR spectrum (a) and Raman spectrum (b) of PEDOT:PSS

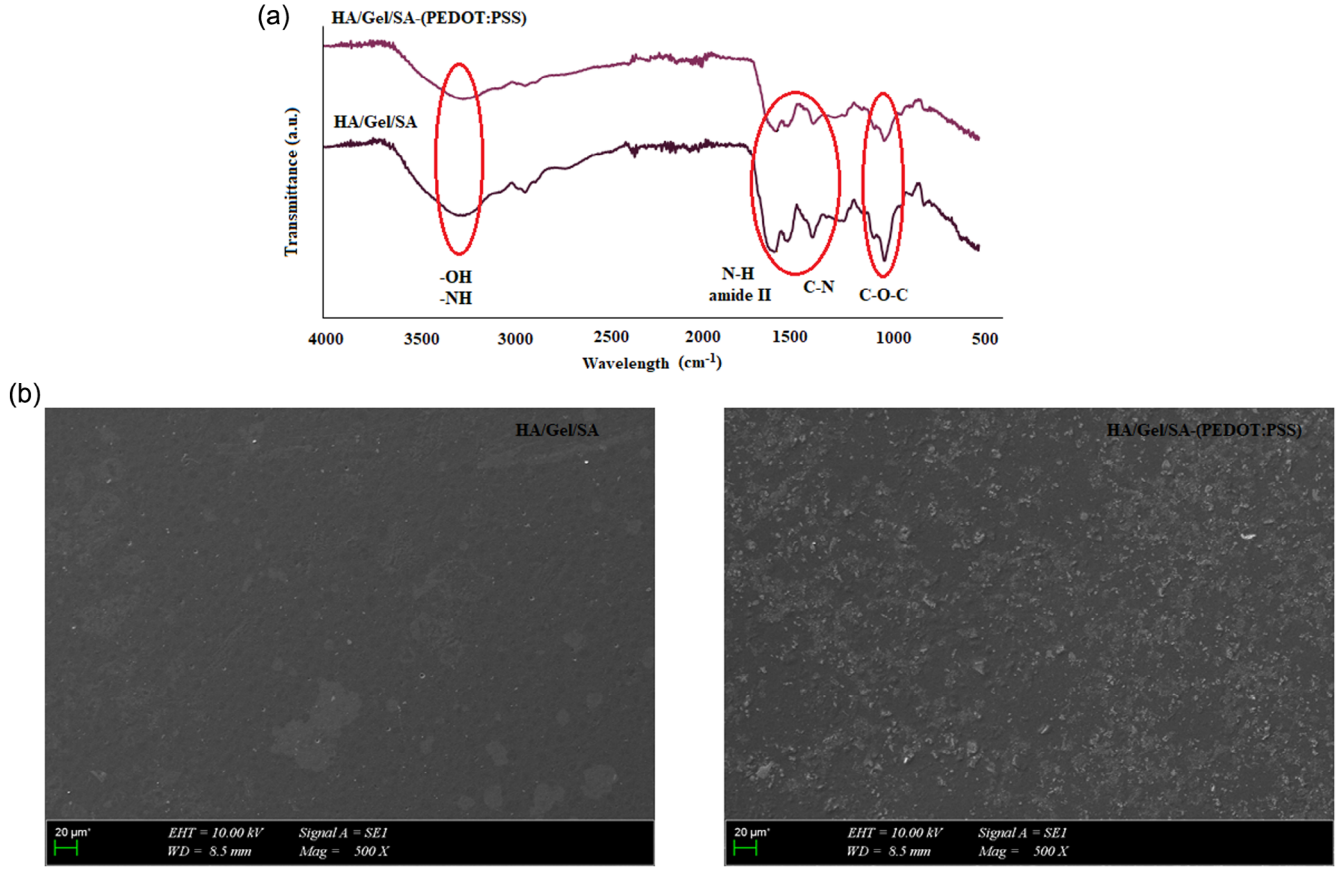

FIGURE 5 FT-IR spectra (a) and SEM images (b) of HA/gel/SA and HA/gel/SA-(PEDOT:PSS) polymeric films [Color figure can be viewed at wileyonlinelibrary.com]

3.3 | Characterization

The chemical structure of PEDOT:PSS was characterized by FT-IR analysis and RAMAN spectroscopy. In the FT-IR spectrum of PEDOT:PSS (Figure 4a), the peaks at 1635 and 1400 cm^{-1} represent C—C and C═C stretching vibrations of the quinoidal structure of the thiophene ring, respectively.[71,72] The bands appeared at 825 and 655 cm^{-1} are associated with the C—S stretching of the thiophene ring. Additionally, the intense peak at 1035 cm^{-1} corresponded to the stretching vibrations of C—O—C in the ethylenedioxy group.[72] While the peak

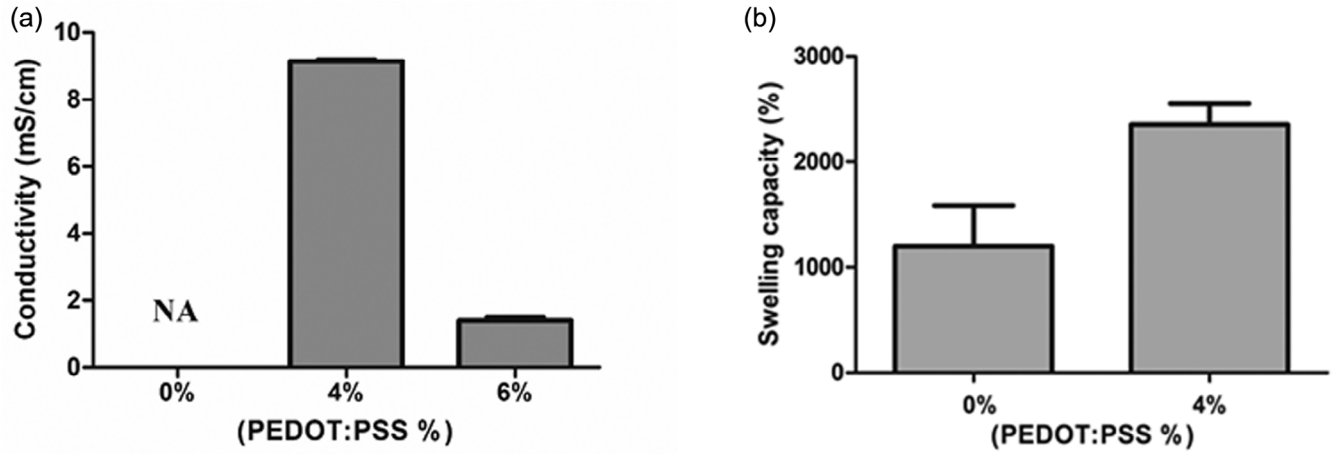

FIGURE 6 Electrical conductivity (a) and swelling capacity (b) of the HA/gel/SA-(PEDOT:PSS) polymeric films

located at 1185 cm^{-1} was assigned to the asymmetric and symmetric vibrations of S—O in sulfonate groups of PSS chains, the S—C phenyl bond in sulfonic acid was observed at 1060 cm^{-1}.[73–75] Figure 4b shows the Raman spectrum of PEDOT:PSS. As shown in the spectrum, the major characteristic bands of PEDOT:PSS structure appeared at between 900 and 1600 cm^{-1}. The peaks at 1280, 1438, and 1500 cm^{-1} were attributed to C_α- C_α' inter-ring stretching, $C_\alpha = C_\beta$ symmetric stretching and $C_\alpha = C_\beta$ asymmetric stretching vibrations of PEDOT:PSS, respectively.[76,77] The vibrational modes of PSS were observed at 984, 1150, and 1575 cm^{-1}.[78–80] All these results confirm that PEDOT:PSS was synthesized successfully.

The FT-IR spectra of HA/Gel/SA and HA/Gel/SA-(PEDOT:PSS) films are depicted in Figure 5a. The characteristic peaks coming from HA, Gel, and SA structures were observed in both spectra. As shown in both spectra, the peaks at 3260 cm^{-1} (—OH and —NH stretching), 1027 cm^{-1} (C—O—C stretching), 1600 cm^{-1} (N—H bending of amide II), 1400 cm^{-1} (COO^- stretching), and 1536 cm^{-1} (C—N stretching) confirm the HA/Gel/SA polymeric network structure.[43,81] In comparison with the FT-IR spectrum of HA/Gel/SA-(PEDOT:PSS) film, the bands appearing at 3250, 2900, 1600, and 1536 cm^{-1} in the spectrum of HA/Gel/SA film were decreased. It could be explained by the forming of hydrogen bonds between the —S groups of PEDOT:PSS and hydroxyl or carboxyl groups of the polymeric network.[27,52,82] Besides, the slight shifting of the peaks to lower regions at around 1400 cm^{-1} is mainly related to the interaction between positively charged groups of the PEDOT:PSS and negatively charged groups of the polymeric network.[83]

A SEM analysis was performed to observe the surface morphologies of the polymeric films. As seen from Figure 5b, PEDOT:PSS particles were homogenously distributed through the polymeric network, which had a quite smooth surface before the incorporation of the PEDOT:PSS into the structure.

3.4 | Electrical conductivity of HA/gel/SA-(PEDOT:PSS) films

The electrical conductivity of the polymeric films was measured by using a four-point probe technique and the results are shown in Figure 6a. Electrical conductivity property was provided with the incorporation of PEDOT:PSS into the polymeric network. The highest electrical conductivity was found as 9.2×10^{-3} S/cm for HA/Gel/SA- 4 v% (PEDOT:PSS) owing to uniform dispersion of PEDOT:PSS in polymeric network and continuous electron transporting path which creates by PSS chains in the structure.[84,85] Since the human body has low microcurrent intensity, this result is accepted as an efficient value, which is in the range of semiconductors (10^{-2}–10^{-6} S/m).[86,87] As seen from Figure 6a, the conductivity value decreased with an increase in the PEDOT:PSS amount from 4 to 6 v%. This decrease could be attributed to the agglomeration of PEDOT:PSS molecules within the polymeric network, which prevents homogenous distribution and reduces electron mobility. Therefore, polymeric films with 4 v% of PEDOT:PSS was considered the most favorable candidate for the targeted application field and the other tests were performed using this formulation.

3.5 | Swelling properties

The swelling behavior of HA/Gel/SA and HA/Gel/SA-4 v% (PEDOT:PSS) polymeric films was investigated in

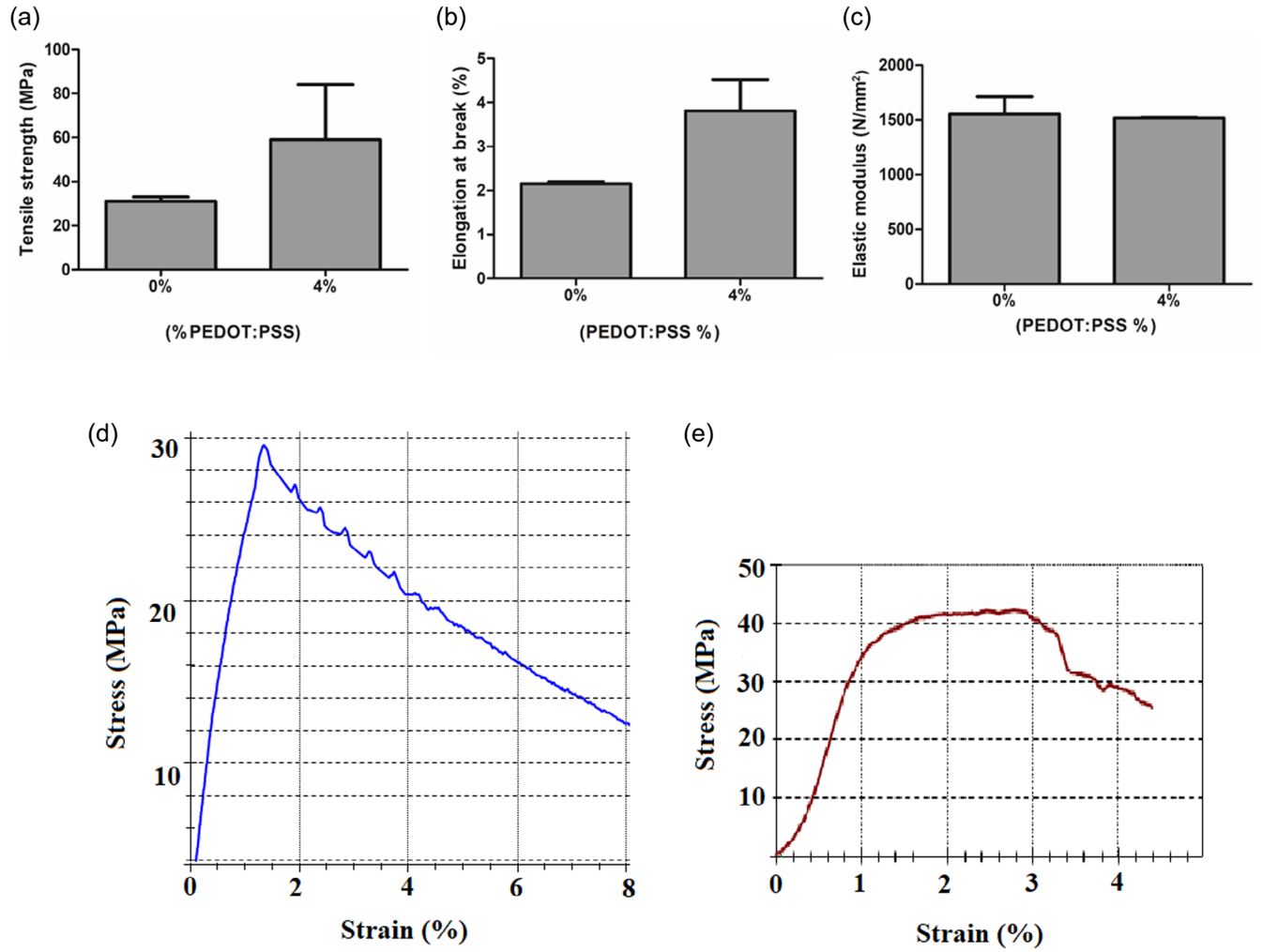

FIGURE 7 Tensile strength (a), elongation at break (b) and elastic modulus (c) of HA/gel/SA and HA/gel/SA-(PEDOT:PSS) polymeric films, stress–strain curves of HA/gel/SA (d) and HA/gel/SA-(PEDOT:PSS) (e) polymeric films [Color figure can be viewed at wileyonlinelibrary.com]

PBS medium at 37°C. While the hydrophilic nature of each component in the polymeric network ensured a good swelling trend for pure film, the swelling capacity additionally increased with the incorporating of PEDOT:PSS into the structure in a good extent (Figure 6b). This phenomenon probably lies in the presence of highly hydrophilic sulfonic acid groups of PSS part in the PEDOT:PSS structure.[88] Furthermore, the addition of PEDOT:PSS into the structure may have reduced the crosslinking density of the polymeric network, resulting in an increment of the water uptake capacity of the polymeric structure.

3.6 | Mechanical performance

Mechanical properties are considered one of the crucial requirements in controlled drug release applications, as high mechanical stability provides protection to the integrity of the drug carrier until reaching the desired region. Actually, the usage of Gel in the ternary composition reinforced the mechanical performance of the films by creating a tough and physically-crosslinked network. In addition to these, the effect of PEDOT:PSS incorporation on mechanical performance was evaluated regarding elastic modulus, tensile strength and elongation at break. As shown in Figure 7, while incorporation of PEDOT:PSS into the structure has no any contribution on the elastic modulus of polymeric films, since PEDOT:PSS into a structure makes the material stiffer and tougher, both tensile strength and elongation at break values increased considerably by incorporating PEDOT:PSS into the structure because of the stiff nature of PEDOT:PSS.[52,82] Furthermore, the formation of hydrogen bonding between functional groups of PEDOT:PSS and polymeric network makes the structure stronger, which results in the

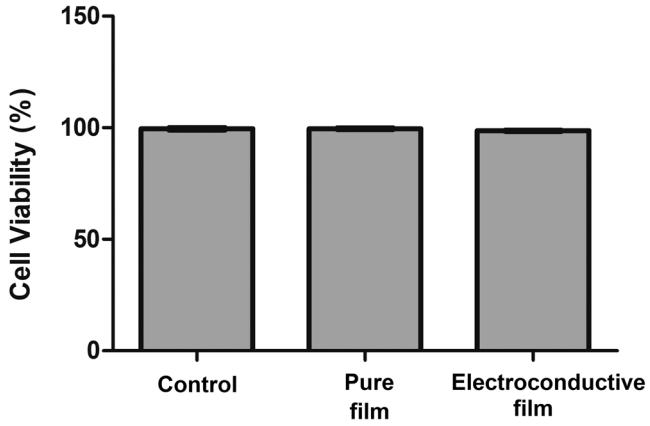

FIGURE 8 In vitro proliferation of L929 cells on HA/gel/SA and HA/gel/SA-(PEDOT:PSS) polymeric films and polystyrene well (control sample)

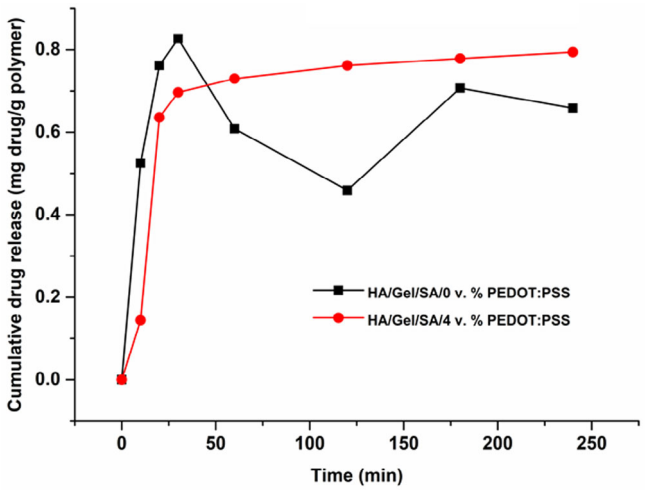

FIGURE 9 Controlled release behavior of CIP from HA/gel/SA and HA/gel/SA-4 v% (PEDOT:PSS) polymeric films [Color figure can be viewed at wileyonlinelibrary.com]

improved mechanical stability. On the other hand PEDOT:PSS could not contribute to the elastic modulus. This contribution of PEDOT:PSS on the mechanical performance could be also seen from the typical stress–strain curves of pure film and PEDOT:PSS based film given in Figure 7. Adding of PEDOT:PSS to the structure enhanced mechanical parameters including tensile strength and stress at yield compared to pure film. According to these results, HA/Gel/SA-4 v% (PEDOT:PSS) polymeric film exhibits acceptable mechanical performance required for the favorable functionality of the drug carrier.[54,89,90]

3.7 | Cytotoxicity tests

The cytotoxic effect of HA/Gel/SA and HA/Gel/SA-(PEDOT:PSS) polymeric films on the L929 cells was investigated by using WST-1 assay. As shown in Figure 8, the cell viability (%) of the each sample was found to be almost 99% owing to non-toxic and biocompatible nature of the each component in the polymeric network. There results demonstrates that the interaction between the produced polymeric films and cell was agreeable, which had good cytocompatibility. The high cell viability value of PEDOT:PSS containing polymeric films might be related to the binding properties of PEDOT:PSS incorporated surfaces, that precisely effect cell adhesion.[91,92]

3.8 | Drug loading and in vitro release studies

In vitro release behaviors of CIP from HA/Gel/SA and HA/Gel/SA- 4 v% (PEDOT:PSS) polymeric films were carried out at pH 7.4, 37°C and 130 rpm, resembling the physiological conditions of plasmatic environment.[93] As seen from Figure 9, the CIP release from PEDOT:PSS containing polymeric films occurred in a slower manner. It is worth to mention that while the cumulative drug release of CIP from different formulations occurred within the minutes in the literature, the release from our HA/Gel/SA-(PEDOT:PSS) films took place over a period of hours.[54,57] The cumulative drug release in first 10 min was found as 0.53 and 0.14 mg drug/g polymer from HA/Gel/SA and HA/Gel/SA-(PEDOT:PSS) polymeric films, respectively. It is an obvious evident that the burst release of CIP, which causes the loss a great amount of drug in a short time period, was decreased by the incorporation of PEDOT:PSS into the structure. This case could be explained that the reduction of the voids in the structure with PEDOT:PSS particles provided the prolonged release of drug because of the additional resistance to the fast migration of the drug. In other words, it ensured more favorable medium to retain the drug molecules within the polymeric network. A more controlled release behavior was provided owing to the filler effect of PEDOT:PSS, while the release profile of pure HA/Gel/SA film showed an unstable behavior like successive declines and increments. These results indicate that HA/Gel/SA-(PEDOT:PSS) formulation had a tough network could function as a favorable drug carrier for a sustainable release profile.

4 | CONCLUSION

The HA/Gel/SA-(PEDOT:PSS) conductive polymeric films were successfully fabricated for drug release applications. The incorporation of PEDOT:PSS into the polymeric network made the mechanical performance of the

films better compared to HA/Gel/SA films. The prepared HA/Gel/SA-4 v% (PEDOT:PSS) film was selected as the optimum composition for the use of an electroconductive drug carrier according to the conductivity test results. Besides, the effect of PEDOT:PSS incorporation on swelling properties and cytotoxicity was observed. The drug release experiment results revealed that the burst release of the drug was reduced and the release behavior of CIP became slower and more controlled manner by the addition of PEDOT:PSS into the polymeric network. Consequently, these results demonstrated that HA/Gel/SA-(PEDOT:PSS) conductive polymeric films with enhanced mechanical performance and good cytocompatibility could be employed as an effective carrier for the model antibiotic drug CIP, which was selected with the aim of treating bacterial infections.

AUTHOR CONTRIBUTIONS

Didem Aycan: Data curation (lead); investigation (equal); methodology (equal); writing – original draft (equal). **Nihal Dolapçı:** Data curation (equal); methodology (equal). **Özge Gülüzar Karaca:** Data curation (equal); methodology (equal). **Neslihan Alemdar:** Conceptualization (lead); data curation (equal); investigation (equal); methodology (equal); resources (lead); supervision (lead); validation (lead); visualization (lead); writing – original draft (equal).

ACKNOWLEDGMENTS

The authors would like to thank the Faculty of Engineering, Marmara University, Turkey for providing all the equipment used for the experiments in this research.

DATA AVAILABILITY STATEMENT

The data that support the findings of this study are available from the corresponding author upon reasonable request.

ORCID

Neslihan Alemdar https://orcid.org/0000-0003-4952-7260

REFERENCES

[1] G. Kaur, R. Adhikari, P. Cass, M. Bown, P. Gunatillake, *RSC Adv.* **2015**, *5*, 37553.
[2] N. K. Guimard, N. Gomez, C. E. Schmidt, *Prog. Polym. Sci.* **2007**, *32*, 876.
[3] D. Aycan, N. A. Yayla, Y. A. Aydin, *Polym. Degrad. Stab.* **2020**, *181*, 109346.
[4] S. Oktay, N. Alemdar, *J. Appl. Polym. Sci.* **2019**, *136*, 46914.
[5] J. G. Hardy, J. Y. Lee, C. E. Schmidt, *Curr. Opin.* **2013**, *24*, 847.
[6] D. Kaya, N. Alemdar, *J. Appl. Polym. Sci.* **2019**, *136*, 46905.
[7] S. Wang, S. Guan, J. Wang, H. Liu, T. Liu, X. Ma, Z. Cui, *J. Biosci. Bioeng.* **2017**, *123*, 116.
[8] H. Torabi, M. Mehdikhani, J. Varshosaz, F. Shafiee, *J. Appl. Polym. Sci.* **2021**, *138*, 50327.
[9] C. A. Chapman, E. A. Cuttaz, J. A. Goding, R. A. Green, *Appl. Phys. Lett.* **2020**, *116*, 010501.
[10] Y. Yun, H. Wu, J. Gao, W. Dai, L. Deng, O. Lv, Y. Kong, *Mater. Sci. Eng., C* **2020**, *108*, 110380.
[11] H. Hu, X. Zhong, S. Yang, H. Fu, *Composites, Part B* **2020**, *182*, 107623.
[12] X.-X. Wang, G.-F. Yu, J. Zhang, M. Yu, S. Ramakrishna, Y.-Z. Long, *Prog. Mater. Sci.* **2021**, *115*, 100704.
[13] C. Alemán, B. Teixeira-Dias, D. Zanuy, F. Estrany, E. Armelin, L. J. Del Valle, *Polym. J.* **2009**, *50*, 1965.
[14] M. Asplund, E. Thaning, J. Lundberg, *Biomed. Mater.* **2009**, *4*, 045009.
[15] R. Balint, N. Cassidy, S. Cartmell, *Acta Biomater.* **2014**, *10*, 2341.
[16] D. Kim, *Acta Biomater.* **2010**, *6*, 57.
[17] L. Groenendaal, F. Jonas, D. Freitag, H. Pielartzik, J. R. Reynolds, *Adv. Mater.* **2000**, *12*, 481.
[18] S. Kirchmeyer, K. Reuter, *J. Mater. Chem.* **2005**, *15*, 2077.
[19] K. R. Reddy, H. M. Jeong, Y. Lee, A. V. Raghu, *J. Polym. Sci. A* **2010**, *48*, 1477.
[20] D. Mantione, I. Del Agua, A. Sanchez-Sanchez, D. Mecerreyes, *Polymer* **2017**, *9*, 354.
[21] R. Lv, Y. Sun, F. Yu, H. Zhang, *J. Appl. Polym. Sci.* **2012**, *124*, 855.
[22] S. Ganguly, P. P. Maity, S. Mondal, P. Das, P. Bhawal, S. Dhara, N. C. Das, *Mater. Sci. Eng. C* **2018**, *92*, 34.
[23] S. Ganguly, D. Ray, P. Das, P. P. Maity, S. Mondal, V. Aswal, S. Dhara, N. C. Das, *Ultrason. Sonochem.* **2018**, *42*, 212.
[24] X. Qi, W. Wei, J. Li, T. Su, X. Pan, G. Zuo, J. Zhang, W. Dong, *Mater. Sci. Eng. C* **2017**, *75*, 487.
[25] K. Tonsomboon, A. L. Butcher, M. L. Oyen, *Mater. Sci. Eng. C* **2017**, *72*, 220.
[26] L. Lapcýk Jr., L. Lapcýk, S. De Smedt, J. Demeester, P. Chabrecek, *Chem. Rev.* **1998**, *98*, 2663.
[27] W. Wang, M. Cui, Z. Song, X. Luo, *RSC Adv.* **2016**, *6*, 88411.
[28] S. Yamanlar, S. Sant, T. Boudou, C. Picart, A. Khademhosseini, *Biomaterials* **2011**, *32*, 5590.
[29] R. Huang, X. Liu, H. Ye, R. Su, W. Qi, L. Wang, Z. He, *Langmuir* **2015**, *31*, 12061.
[30] S. Jiang, Z. Cao, *Adv. Mater.* **2010**, *22*, 920.
[31] C. Leng, H.-C. Hung, S. Sun, D. Wang, Y. Li, S. Jiang, Z. Chen, *ACS Appl. Mater. Interfaces* **2015**, *7*, 16881.
[32] M. C. Lukowiak, S. Wettmarshausen, G. Hidde, P. Landsberger, V. Boenke, K. Rodenacker, U. Braun, J. F. Friedrich, A. A. Gorbushina, R. Haag, *Polym. J.* **2015**, *6*, 1350.
[33] Q. Shi, Y. Su, W. Chen, J. Peng, L. Nie, L. Zhang, Z. Jiang, *J. Membr. Sci.* **2011**, *366*, 398.
[34] A. D. White, A. K. Nowinski, W. Huang, A. J. Keefe, F. Sun, S. Jiang, *Chem. Sci.* **2012**, *3*, 3488.
[35] I. S. Bayer, *Molecules* **2020**, *25*, 2649.
[36] N. Alemdar, *Carbohydr. Polym.* **2016**, *151*, 1019.
[37] D. Aycan, B. Selmi, E. Kelel, T. Yildirim, N. Alemdar, *Eur. Polym. J.* **2019**, *121*, 109308.
[38] Y. Liu, X. Z. Shu, G. D. Prestwich, *Biomaterials* **2005**, *26*, 4737.
[39] H.-Y. Lee, H.-E. Kim, S.-H. Jeong, *Colloids Surf., B* **2019**, *174*, 308.
[40] Y. Minaberry, D. A. Chiappetta, A. Sosnik, M. Jobbagy, *Biomacromolecules* **2013**, *14*, 1.

[41] D. Nguyen, A. Hui, A. Weeks, M. Heynen, E. Joyce, H. Sheardown, L. Jones, *Materials* **2012**, *5*, 684.
[42] D. Kaya, K. Küçükada, N. Alemdar, *Carbohydr. Polym.* **2019**, *215*, 189.
[43] Z. Zhou, J. Chen, C. Peng, T. Huang, H. Zhou, B. Ou, J. Chen, Q. Liu, S. He, D. Cao, *J. Macromol. Sci. A* **2014**, *51*, 318.
[44] Y. Li, J. Rodrigues, H. Tomas, *Chem. Sci.* **2012**, *41*, 2193.
[45] D. Olsen, C. Yang, M. Bodo, R. Chang, S. Leigh, J. Baez, D. Carmichael, M. Perälä, E.-R. Hämäläinen, M. Jarvinen, *Adv. Drug Delivery Rev.* **2003**, *55*, 1547.
[46] S. A. Sell, M. J. McClure, K. Garg, P. S. Wolfe, G. L. Bowlin, *Adv. Drug Delivery Rev.* **2009**, *61*, 1007.
[47] L. Sui, B. Peng, S. Huang, Y. Wang, L. Ju, *J. Wuhan Univ. Technol. Mater. Sci. Ed. J.* **2016**, *31*, 662.
[48] S. Young, M. Wong, Y. Tabata, A. G. Mikos, *J. Controlled Release* **2005**, *109*, 256.
[49] M. Jurga, M. B. Dainiak, A. Sarnowska, A. Jablonska, A. Tripathi, F. M. Plieva, I. N. Savina, L. Strojek, H. Jungvid, A. Kumar, *Biomaterials* **2011**, *32*, 3423.
[50] E. Martín-López, F. R. Alonso, M. Nieto-Díaz, M. Nieto-Sampedro, *J. Biomater. Sci. Polym. Ed.* **2012**, *23*, 207.
[51] E. Martín-López, M. Nieto-Díaz, M. Nieto-Sampedro, *J. Biomater. Appl.* **2012**, *26*, 791.
[52] S. Wang, S. Guan, Z. Zhu, W. Li, T. Liu, X. Ma, *Mater. Sci. Eng. C* **2017**, *71*, 308.
[53] S. Bozdag, K. Dillen, J. Vandervoort, A. Ludwig, *J. Pharm. Pharmacol.* **2005**, *57*, 699.
[54] M. Contardi, J. A. Heredia-Guerrero, G. Perotto, P. Valentini, P. P. Pompa, R. Spanò, L. Goldoni, R. Bertorelli, A. Athanassiou, I. S. Bayer, *Eur. J. Pharm. Sci.* **2017**, *104*, 133.
[55] S. Ghaffari, J. Varshosaz, I. Haririan, M. R. Khoshayand, S. Azarmi, T. Gazori, *J. Dispersion Sci. Technol.* **2012**, *33*, 685.
[56] D. Jain, R. Banerjee, *J. Biomed. Mater. Res. B* **2008**, *86*, 105.
[57] S. Sharmeen, A. M. Rahman, M. M. Lubna, K. S. Salem, R. Islam, M. A. Khan, *Bioact. Mater.* **2018**, *3*, 236.
[58] J. S. Boateng, K. H. Matthews, H. N. Stevens, G. M. Eccleston, *J. Pharm. Sci.* **2008**, *97*, 2892.
[59] B. K. Heragh, S. Javanshir, G. R. Mahdavinia, M. R. N. Jamal, *Int. J. Biol. Macromol.* **2021**, *190*, 351.
[60] N. Hosseini-Ashtiani, A. Tadjarodi, R. Zare-Dorabei, *Int. J. Biol. Macromol.* **2021**, *176*, 459.
[61] M. S. Sarwar, A. Ghaffar, Q. Huang, *Polym. Polym. Compos.* **2021**, *29*, S143.
[62] M. S. Sarwar, A. Ghaffar, Q. Huang, M. S. Zafar, M. Usman, M. Latif, *Int. J. Biol. Macromol.* **2020**, *165*, 1047.
[63] M. S. Sarwar, Q. Huang, A. Ghaffar, M. A. Abid, M. S. Zafar, Z. Khurshid, M. Latif, *Pharmaceutics* **2020**, *12*, 131.
[64] I. Sengupta, S. S. S. Kumar, K. Gupta, S. Chakraborty, *Mater. Today Commun.* **2021**, *26*, 101737.
[65] I. Miccoli, F. Edler, H. Pfnür, C. Tegenkamp, *J. Condens. Matter. Phys.* **2015**, *27*, 223201.
[66] D. Aycan, N. Alemdar, *Carbohydr. Polym.* **2018**, *184*, 401.
[67] Y. S. Kim, K. Cho, H. J. Lee, S. Chang, H. Lee, J. H. Kim, W.-G. Koh, *React. Funct. Polym.* **2016**, *109*, 15.
[68] E. J. Choi, J. Shin, Z. H. Khaleel, I. Cha, S.-H. Yun, S.-W. Cho, C. Song, *Polym. Chem.* **2015**, *6*, 4473.
[69] A. B. Sanghvi, K. P.-H. Miller, A. M. Belcher, C. E. Schmidt, *Nat. Mater.* **2005**, *4*, 496.
[70] B. Cohen, A. Shefy-Peleg, M. Zilberman, *J. Biomater. Sci. Polym. Ed.* **2014**, *25*, 224.
[71] Y. Chen, J. Xu, Y. Yang, Y. Zhao, W. Yang, X. Mao, X. He, S. Li, *Electrochim. Acta* **2016**, *193*, 199.
[72] M. Lay, M. À. Pèlach, N. Pellicer, J. A. Tarrés, K. N. Bun, F. Vilaseca, *Carbohydr. Polym.* **2017**, *165*, 86.
[73] Q. Jiang, C. Liu, H. Song, J. Xu, D. Mo, H. Shi, Z. Wang, F. Jiang, B. Lu, Z. Zhu, *Int. J. Electrochem. Sci.* **2014**, *9*, 7540.
[74] S. Khan, M. Ul-Islam, W. A. Khattak, M. W. Ullah, J. K. Park, *Carbohydr. Polym.* **2015**, *127*, 86.
[75] Z. Zhu, H. Song, J. Xu, C. Liu, Q. Jiang, H. Shi, *J. Mater. Sci. Mater.* **2015**, *26*, 429.
[76] W. W. Chiu, J. Travaš-Sejdić, R. P. Cooney, G. A. Bowmaker, *J. Raman Spectrosc.* **2006**, *37*, 1354.
[77] S. Xiong, L. Zhang, X. Lu, *Polym. Bull.* **2013**, *70*, 237.
[78] A. A. Farah, S. A. Rutledge, A. Schaarschmidt, R. Lai, J. P. Freedman, A. S. Helmy, *J. Appl. Phys.* **2012**, *112*, 113709.
[79] S. Garreau, J. Duvail, G. Louarn, *Synth. Met.* **2001**, *125*, 325.
[80] Y.-K. Han, M.-Y. Chang, W.-Y. Huang, H.-Y. Pan, K.-S. Ho, T.-H. Hsieh, S.-Y. Pan, *J. Electrochem. Soc.* **2011**, *158*, K88.
[81] M. Lian, J. Fan, Z. Shi, S. Zhang, H. Li, J. Yin, *Carbon* **2015**, *89*, 279.
[82] S. Wang, C. Sun, S. Guan, W. Li, J. Xu, D. Ge, M. Zhuang, T. Liu, X. Ma, *J. Mater. Chem. B* **2017**, *5*, 4774.
[83] M. Rajkumar, N. Meenakshisundaram, V. Rajendran, *Mater. Charact.* **2011**, *62*, 469.
[84] R. K. Pal, E. E. Turner, B. H. Chalfant, V. K. Yadavalli, *React. Funct. Polym.* **2017**, *120*, 66.
[85] M. Zahid, E. L. Papadopoulou, A. Athanassiou, I. S. Bayer, *Mater. Des.* **2017**, *135*, 213.
[86] J.-W. Lee, F. Serna, J. Nickels, C. E. Schmidt, *Biomacromolecules* **2006**, *7*, 1692.
[87] J. Niple, J. Daigle, L. Zaffanella, T. Sullivan, R. Kavet, *Bioelectromagnetics* **2004**, *25*, 369.
[88] B. Lu, H. Yuk, S. Lin, N. Jian, K. Qu, J. Xu, X. Zhao, *Nat. Commun.* **2019**, *10*, 1.
[89] S. Ghalei, H. Asadi, B. Ghalei, *J. Appl. Polym. Sci.* **2018**, *135*, 46643.
[90] S. Shankar, J.-W. Rhim, *Food Hydrocolloids* **2018**, *82*, 116.
[91] S.-C. Luo, *Polym. Rev.* **2013**, *53*, 303.
[92] H. Zhao, B. Zhu, S.-C. Luo, H.-A. Lin, A. Nakao, Y. Yamashita, H.-H. Yu, *ACS Appl. Mater. Interfaces* **2013**, *5*, 4536.
[93] M. C. García, A. A. Aldana, L. I. Tártara, F. Alovero, M. C. Strumia, R. H. Manzo, M. Martinelli, A. F. Jimenez-Kairuz, *Carbohydr. Polym.* **2017**, *175*, 75.

How to cite this article: D. Aycan, N. Dolapçı, Özge Gülüzar Karaca, N. Alemdar, *J. Appl. Polym. Sci.* **2022**, *139*(32), e52761. https://doi.org/10.1002/app.52761